Modelling a small-scale hydrogen valley: Optimisation under techno-economic and environmental perspectives

International Journal of Hydrogen Energy 191 (2025) 152172

Contents lists available at ScienceDirect

International Journal of Hydrogen Energy

journal homepage: www.elsevier.com/locate/he

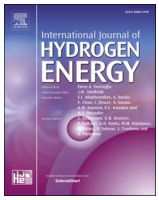

Modelling a small-scale hydrogen valley: Optimisation under techno-economic and environmental perspectives

Vincenzo Romano *, Paolo Marocco, Marta Gandiglio, Massimo Santarelli

Department of Energy, Politecnico di Torino, Corso Duca degli Abruzzi 24, 10129, Torino, Italy

ARTICLE INFO

Handling Editor: Umit Koylu

Keywords:
Hydrogen valley
Green hydrogen
MILP
Hydrogen emissions
Sector coupling
Non-interconnected island

ABSTRACT

Renewable hydrogen is a promising pathway to decarbonise hard-to-electrify sectors, though its widespread deployment remains hindered by economic challenges. Hydrogen valleys, integrated regional systems, have emerged as a strategic solution to scale up hydrogen infrastructure and demand. This study assesses the techno-economic feasibility of a hydrogen valley in southeastern Crete, based on the CRAVE-H_2 project, using a Mixed-Integer Linear Programming (MILP) optimisation model. The system serves multiple end-uses: touristic fuel cell buses and a vessel, as well as cold ironing for ships at berth. In addition to renewable generators, electricity can be supplied via a hybrid storage system or purchased from the grid, with dispatch optimised according to hourly market prices. A customised modelling framework is developed within PyPSA using the Linopy extension, enabling the inclusion of piecewise affine approximations of non-linear performance curves for electrolysers and fuel cells, alongside operating range constraints. Hydrogen leakage is also explicitly modelled to assess its environmental and economic implications. The model delivers optimal component sizing, energy dispatch strategies, and key performance metrics, including Levelised Cost Of Hydrogen (LCOH), aggregated Levelised Cost Of Energy (LCOE) and carbon intensity. Most scenarios yield competitive LCOH values between 5.36 and 8.21 €/kgH_2, increasing to 15 €/kgH_2 under full decarbonisation due to extensive storage investments. Hydrogen emissions, that may exceed 10 % of total production in worst-case scenarios, become more pronounced in fully decarbonised scenarios. These findings underline the importance of emissions tracking and provide practical insights to inform the design of cost-effective, low-emission hydrogen valleys.

1. Introduction

Hydrogen is increasingly recognised as a key enabler of decarbonisation pathways, owing to its flexibility as an energy vector and its ability to interconnect multiple sectors, particularly those that are difficult to electrify and considered hard to abate [1]. Despite a growing interest and numerous announced projects aimed at expanding low-emission hydrogen production, the development of a clean hydrogen economy still faces substantial technical, economic, and policy-related challenges [2].

Among the various government strategies to foster hydrogen deployment, one of the most promising and fast-emerging concepts is that of hydrogen valleys. These are geographically defined hydrogen ecosystems, ranging from industrial zones and urban districts to entire regions or islands, that span the full hydrogen value chain. By integrating multiple applications, hydrogen valleys enhance economic viability and highlight the cross-sector potential of hydrogen-based energy systems [3].

Island contexts in particular can benefit from such configurations. Hydrogen valleys can support high shares of renewable energy sources, provide targeted solutions for port infrastructures, and offer decarbonisation pathways for local transport, especially in tourism-oriented mobility [4].

A comprehensive overview of ongoing hydrogen valley initiatives has been provided by Bamapou et al. [5], complemented by the mapping efforts of the Clean Hydrogen Partnership [6], which catalogues international projects at various stages of development.

1.1. Literature review on hydrogen valley models

1.1.1. Hydrogen valleys in the current modelling framework

Hydrogen valleys are a recent development in the energy sector and energy system modelling. Positioned between detailed plant-level models and large-scale spatial models, they balance technical fidelity

* Corresponding author.
E-mail address: vincenzo.romano@polito.it (V. Romano).

https://doi.org/10.1016/j.ijhydene.2025.152172
Received 9 September 2025; Received in revised form 20 October 2025; Accepted 21 October 2025
Available online 31 October 2025

with manageable spatial and temporal scopes. Unlike large-scale models based on Linear Programming (LP), which require simplifying assumptions for tractability, hydrogen valley models operate at regional or local levels and allow more detailed representations of system components and operational aspects.

Given their novelty, few modelling frameworks exist for hydrogen valleys, and no standardised methodology has emerged. Their hybrid, multi-sectoral nature aligns well with Mixed-Integer Linear Programming (MILP), which enables flexible, yet tractable modelling of discrete operations and approximated non-linear behaviours [7].

While only a few studies explicitly refer to "hydrogen valleys", many reflect their defining features: geographic boundaries, full value chain coverage, and multi-sectoral integration.

1.1.2. Spatially resolved and multi-nodal models

Some of the most advanced studies focus on the spatial and infrastructural configuration of hydrogen supply systems. Mendler et al. [8] developed the HYSCOPE model, a dynamic, spatially resolved optimisation framework that integrates system dynamics with techno-economic analysis. Applied to a German case study, it assesses the effects of spatial resolution, clustering methods, hydrogen exchange mechanisms, and import/export options on performance and cost. This model, which uses a non-linear solver, bridges the gap between large-scale energy modelling and detailed component-level representation.

Similarly, Rosén et al. [9] examined a hydrogen valley formed by three Swedish urban nodes, evaluating the benefits of interconnection via hydrogen pipelines. Their MILP-based model includes investment decisions in infrastructure and models gas dynamics using linearised Euler equations, a feature rarely included in hydrogen-focused optimisation models. Results highlight the role of spatial coordination in lowering costs and improving renewable energy utilisation.

1.1.3. Component-level detail and electrolyser modelling

Other studies emphasise technological detail and component-level modelling. Guichard et al. [10] integrated a reversible solid oxide cell with an offshore wind farm in PyPSA, introducing variable electrolyser efficiency via five discrete points derived from a non-linear curve. Though less detailed than continuous piecewise-linear MILP approximations, this remains the only known PyPSA implementation capturing load-dependent efficiency.

Dadkhah et al. [11] used a Mixed-Integer Non-Linear Programming (MINLP) model to optimise a hydrogen refuelling station system serving fuel cell vehicles and participating in electricity markets. The model incorporates non-linear electrolyser efficiency, grid tariffs, and reserve market dynamics. While not explicitly termed a hydrogen valley, the system spans multiple sectors and value chain stages. Results show that market participation can reduce hydrogen break-even prices, particularly under favourable policy conditions.

1.1.4. Multi-sector integration and valley-scale applications

Several studies examine fully integrated hydrogen valleys across multiple end-use sectors. Petrollese et al. [12] assessed a system in Cagliari, Italy, serving four applications: a stationary fuel cell, hydrogen refuelling station, natural gas grid injection, and biological methanation. Developed in Aspen Plus and coupled with techno-economic analysis, the model evaluates performance under different renewable energy mixes. It is among the few studies including fuel cells as demand sources for electric and thermal loads.

Genovese et al. [13] proposed a virtual hydrogen valley in Calabria, Italy, with centralised hydrogen production distributed via fuel cell hybrid trains to seven refuelling hubs. These serve diverse applications, including buses, forklifts, scooters, a ferry and an aircraft. Their model integrates dynamic train propulsion simulations, infrastructure sizing, and a 10 % hydrogen leakage assumption. Under optimistic conditions, an LCOH as low as 5.4 €/kg is achievable, with emissions reductions of up to 3.2 $ktCO_2eq$/year and €51 million in health benefits.

Port environments also offer potential for hydrogen ecosystems. Conte et al. [14] studied the port of Genova as a multi-energy hub for cold ironing, supplying ships with electricity and hydrogen. Their model includes Photovoltaic (PV) and wind, Battery Energy Storage System (BESS), and a Hydrogen Energy Storage System (HESS) composed of an electrolyser, hydrogen tank, and fuel cell. Using a stochastic model predictive control approach, the system manages dispatch under uncertainty, based on ship schedules and load profiles. Results show full demand coverage, avoided diesel use, and economic gains from shore power services.

1.2. Identified gaps and novelty and aim of the work

Despite growing interest, key gaps remain in current modelling. The role of stationary fuel cells as dispatchable power sources during renewable shortfalls is rarely explored, and hydrogen leakages, despite their environmental relevance due to hydrogen's indirect Global Warming Potential (GWP) [15,16], are scarcely included in techno-economic assessments.

This study aims at addressing the identified gaps through the implementation of the following features:

- This study is directly aligned with the real-world CRAVE-H_2 hydrogen valley project [17], supporting the decarbonisation of Crete through green hydrogen supply to hard-to-abate sectors. The techno-economic analysis simulates system operations and evaluates key performance metrics to guide project design, deployment, and strategic decisions.
- While few studies explore hydrogen valleys serving multiple end users, this work assesses the techno-economic feasibility of supplying green hydrogen for touristic buses, a vessel, and electricity for port cold ironing. It also considers the use of a stationary fuel cell as a backup or complementary power source, making it one of the few analyses to integrate such a component. This enhances the multi-vector nature of the system by extending its role beyond hydrogen supply alone.
- This study introduces an innovative methodological contribution by implementing a continuous Piecewise Affine (PWA) approximation of non-linear, load-dependent performance curves for electrolysers and fuel cells within the PyPSA framework [18]. The formulation also incorporates modulation limits based on minimum operating points, a common feature in MILP environments [19,20]. Achieved through a modified network configuration, this approach departs from PyPSA's standard representation of hydrogen technologies. While PyPSA is widely used for large-scale energy modelling due to its flexibility, open-source nature, and efficient data handling, its default components lack detailed resolution for hydrogen systems. By integrating PyPSA with the Linopy package [21], this work enables greater customisation and accuracy, offering a balance between detail and computational effort.
- Another key contribution of this work is the explicit modelling of hydrogen leakages, both intentional (e.g. venting and purging) and unintentional (e.g. fugitive emissions), along the entire value chain. This feature, largely absent in existing hydrogen system models, allows for more comprehensive environmental assessments, particularly considering hydrogen's global warming potential (GWP) and its indirect effects on atmospheric chemistry [16]. Beyond environmental concerns, the model captures the techno-economic impacts of hydrogen losses. In worst-case scenarios, cumulative emissions can exceed 10 %, depending on system layout, technology type, and operational strategy [15,22], potentially reducing overall efficiency and economic performance. Incorporating these effects supports more realistic evaluations and highlights the importance of mitigation strategies to reduce emissions and related costs.

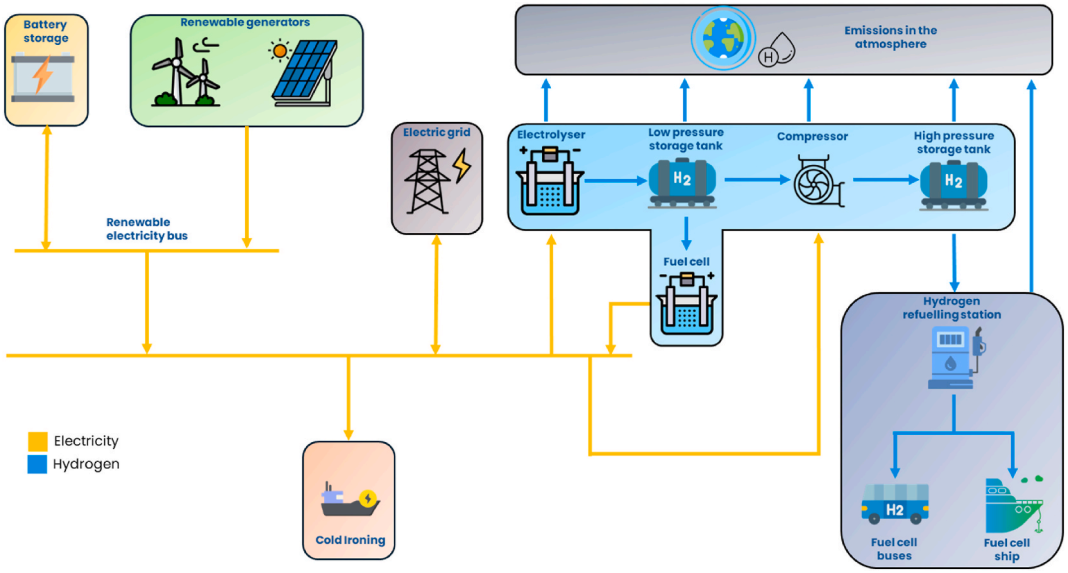

Fig. 1. Scheme of the CRAVE-H_2 hydrogen valley model.

The remainder of this work is structured as follows: Section 2 outlines the methodology adopted for the modelling of the hydrogen valley, detailing the input data used for the case study, as well as the main techno-economic and environmental indicators; Section 3 presents and discusses the results; while key conclusions are summarised in Section 4.

2. Methodology

This section outlines the modelling methodology for simulating the hydrogen valley, which aims at finding the optimal plant configuration and sizing as well as the optimal dispatch of energy flows, simulated across a yearly horizon with hourly timesteps.

The description will cover the presentation of the case study (Section 2.1), plant layout (Section 2.2), implementation within PyPSA modelling framework (Section 2.3), the key objectives and derived KPIs, categorised into techno-economic and environmental indicators (Section 2.4), the simulated scenarios (Section 2.5), and, lastly, the estimated demand profiles together with all the exogenous input data used in the optimisation model (Section 2.6).

2.1. Case study overview

This study analyses a hydrogen valley planned in southeastern Crete, developed under the EU-funded CRAVE-H_2 project [17]. The initiative supports the decarbonisation of the island by producing and distributing hydrogen for multiple applications, while improving the integration of variable renewable energies into the local energy system. The modelled hydrogen-based system targets two main end uses: tourism-oriented mobility, including fuel cell-powered buses and a vessel, and cold ironing for large ships at berth [23].

Given the limited spatial scope of the valley in its initial phase, concentrated around a central hub and aggregated local demand, a spatially zero-dimensional technical-economic optimisation model was developed within a MILP framework.

2.1.1. Energy system in Crete and role of the modelled hydrogen valley

Crete, one of the largest islands in the Mediterranean, has historically operated as an isolated energy system. Despite the island's strong renewable potential, particularly in solar and wind power, which could theoretically meet its total electricity needs, the integration of renewable energy remains limited. This is mainly due to the poor stability of the grid, which hinders the development of additional renewable capacity. As a result, the decarbonisation of Crete depends to a large extent on interconnections with external regions [24]. To overcome this limitation, a high-voltage interconnection with mainland Greece was approved [24–26], with construction recently completed and the line now in operation [27].

In the last few years, where the power system has been operated as a non-interconnected island, renewables (PV, wind, and hydro) contributed slightly over 20 % of Crete's annual electricity consumption, which totals around 3000 GWh with a peak demand of 710 MW. The rest was still met predominantly by oil- and heavy fuel-based power plants [25,28,29].

In this context, the CRAVE-H_2 hydrogen valley not only targets emissions reduction in hard-to-abate sectors but also aligns with Crete's broader energy transition strategy. In the near future, it may serve as a strategic node for two planned interconnections with Egypt and Cyclades archipelago for a large renewable energy harvest [30,31]. These future links, however, are not considered in this study, which focuses on the short-term assessment of the valley's current configuration.

Moreover, the system is modelled as operating on a non-interconnected island. Despite the recent commissioning of the power-line with mainland, assumption enhances the model's relevance to other non-interconnected islands that could benefit from hydrogen-valley deployment.

2.1.2. The role of hydrogen in CRAVE-H_2 end-use sectors

Within the evolving energy landscape outlined above, hydrogen plays a key role in supporting decarbonisation across strategic sectors, offering a complementary pathway to renewable electrification. Its use is particularly valuable in energy-intensive applications where battery-electric solutions face technical or operational limitations.

Hydrogen is widely recognised as a clean fuel with strong potential in heavy-duty transport, such as buses and trucks, thanks to its high energy density. This enables longer driving ranges and shorter refuelling times compared to battery-electric alternatives [1]. However, the large-scale deployment of fuel cell technologies in transport remains contingent on long-term policy support to ensure economic viability [32].

Beyond road transport, hydrogen is also emerging as a decarbonisation solution for ports and maritime operations. It offers a cleaner substitute for diesel and bunker fuel, both in auxiliary power systems and propulsion [33]. Several studies underline the environmental benefits and potential cost competitiveness of hydrogen-based marine

propulsion [34–36].

One relevant application is cold ironing, i.e. supplying electricity from shore to docked ships, allowing them to switch off their on-board diesel generators. Although effective in reducing port emissions [37, 38], cold ironing requires significant electrical capacity, which can put a strain on local grids. This is particularly problematic in areas such as Crete, where grid stability remains a major challenge. Furthermore, in areas with a carbon-intensive electricity mix, as in the case of Crete, cold ironing may offer only limited environmental benefits, also given its costly infrastructure requirements [39]. One alternative examined in this study involves the use of stationary fuel cells powered by locally produced green hydrogen for cold ironing. This approach improves environmental performance while reducing dependence on the electricity grid, an important factor in the analysed context.

These considerations are particularly relevant given the economic weight of tourism and port activities on the island, which make their decarbonisation a strategic priority for Crete's broader energy transition.

2.2. System layout

The modelled system is based on the actual layout of the CRAVE-H_2 valley, reflecting the hydrogen end-uses described in previous sections, and includes the following key components:

- A PV plant and a wind farm, supported by a BESS, forming the renewable power generation node;
- Crete's electric grid, allowing for both import and export of electricity;
- A hydrogen production and gaseous storage chain, composed of an electrolyser, a Low-Pressure Storage Tank (LPST), a compressor, and a High-Pressure Storage Tank (HPST);
- A Hydrogen Refuelling Station (HRS) for end-use distribution, supplied by the HPST;
- A stationary fuel cell unit, fed by the LPST.

Fig. 1 illustrates the valley scheme, together with the end uses of hydrogen and electricity. Further details on demand profiles are provided in Section 2.6.1.

To minimise the use of grid electricity, which remains largely reliant on fossil fuel-based generation, and thereby reduce associated CO_2-eq emissions, the system employs hybrid storage solutions, namely the BESS and the LPST buffer connected to the fuel cell, to meet the electric demand during periods of low renewable generation. The model's reliance on grid electricity or storage is driven by its optimisation objectives: it tends to favour grid use based on purely economic perspectives, while shifting toward storage solutions when environmental constraints are imposed. Moreover, excess energy from renewable generators can be sold to the grid to improve the profitability of the system. Finally, specific hydrogen leakage rates are associated to several components, namely the electrolyser, the compressor, the HRS, the two storage tanks and the fuel cell.

2.3. Modelling implementation in PyPSA

The model is developed within a MILP framework, using the Python-based library PyPSA [18], which is originally formulated for LP. To accommodate mixed-integer features, PyPSA is coupled with the Linopy library [21].

The system is modelled using PyPSA's standard component formulations [40], where core elements such as buses, links, and storage units were implemented according to the native definitions provided by the tool.

However, specific adaptations are introduced for the electrolyser and fuel cell components to more accurately represent their technical behaviour and operational constraints within the hydrogen valley context. These custom features are described in the following subsections.

The PyPSA default components are employed as follows:

- Generators: representing the PV field, wind farm, and the electricity grid;
- Links: modelling the electrolyser, fuel cell, pipelines, powerlines, compressor, and HRS dispenser;
- Stores: representing LPST and HPST;
- Storage Units: representing the BESS.

The objective function is formulated to minimise the total annualised cost $C_{A,tot}$ (in M€/year) of the system, as follows:

$$f_{obj} = \min \left\{ C_{A,tot} \right\} \tag{1}$$

The $C_{A,tot}$ parameter is calculated as the sum of the annualised cost contributions from all i-th components:

$$C_{A,tot} = \sum_i C_{NPC_i} = \sum_i \left(C_{CAPEX_i} \cdot CRF_i + C_{FOM_i} + C_{VOM_i} + C_{ARC_i} \right) \tag{2}$$

The various contributors appearing in Eq. (2) are defined as:

$$C_{CAPEX_i} = c_{CAPEX_i} \cdot S_i \tag{3}$$

$$CRF_i = \frac{r}{1 - (1+r)^{-n_i}} \tag{4}$$

$$C_{FOM_i} = c_{FOM_i} \cdot S_i \tag{5}$$

$$C_{VOM_i} = \sum_t^T c_{VOM_i} \cdot P_i(t) \cdot \Delta t \tag{6}$$

$$C_{ARC_i} = \left(c_{RC_i} \cdot \sum_{RY_i} \frac{r}{1 - (1+r)^{-RY_i}} \right) \cdot S_i \tag{7}$$

where:

- c_{CAPEX_i} is the specific investment cost for component i, in €/kW for most components and in €/kWh for storage units (BESS, LPST and HPST). The total Capital Expenditure (CAPEX) for component i, C_{CAPEX_i}, is obtained by multiplying c_{CAPEX_i} by the installed component size S_i.
- c_{FOM_i} is the specific fixed Operation and Maintenance (O&M) cost, typically expressed as a percentage of the capital cost. The resulting fixed O&M cost is denoted as C_{FOM_i}.
- $c_{VOM_i}(t)$ is the variable O&M cost, which depends on the energy flow and thus varies over time. To compute the total cost contribution C_{VOM_i}, the specific cost is multiplied by the total energy consumed, which is obtained by integrating the power profile $P_i(t)$ over time steps Δt across the entire time horizon T (set to 8760 h). This cost term is used in the model to account for electricity purchases from the grid.
- CRF is the capital recovery factor, used to annualise capital and replacement costs. It is a function of the interest rate r and the component lifetime n (in years).
- C_{ARC_i} represents the annualised replacement costs, which is non-zero only for the electrolyser, fuel cell and BESS. This term accounts for the replacements of the stack (for the electrolyser and fuel cell) and module (for the BESS) occurring during the project lifetime. It is calculated based on the replacement year RY_i of component i and the specific stack/module replacement cost c_{RC_i}, expressed as a percentage of the component's specific capital cost. Under current assumptions, stack replacements for the electrolyser and fuel cell are scheduled to occur twice during the project lifetime, every 7 years, while the BESS is assumed to be replaced once, in year 10.

Table 1
Upper and lower leakage rate (% mass) estimates by component [15].

Component	Lower leakage rate [%]	Upper leakage rate [%]
Electrolyser[a]	0.1 %	9.2 %
Compressor[b]	0.14 %	0.27 %
HRS[b]	1 %	3 %
Storage tanks[c]	0.005 %/h	0.01 %/h

[a] % referred to the output flow.
[b] % referred to the input flow.
[c] % referred to of the amount of hydrogen stored per hour [44].

The terms C_{FOM_i}, C_{VOM_i} and C_{ARC_i} constitute together the total Operational Expenditure (OPEX) of each component *i*.

Given the objective function (i.e., minimisation of the total annualised cost), the optimisation computes the cost-optimal hourly dispatch that meets all demands while sizing all components. No exogenous capacity bounds are imposed, meaning that all components can be freely invested in at the size that best serves the cost-minimisation objective.

It should be noted that the objective function is formulated without accounting for revenues from excess electricity export. This approach is intended to discourage disproportionate investments in renewable capacity that would otherwise prioritise electricity export over hydrogen production and cold ironing supply. To assign a value to excess renewable energy, treated as curtailed from the optimisation perspective, a post-processing step multiplies this amount by a fixed price, simulating its sale to the grid in accordance with the current Greek Feed-in Tariff (FIT) scheme for RES plants on non-interconnected islands such as Crete [41]. This method enables a realistic economic valorisation of surplus renewable energy without influencing the optimisation process of the hydrogen-centred energy system, as also applied in Ref. [42].

2.3.1. Electrolyser and fuel cell modelling

The reduced spatial scope of the model compared to typical PyPSA applications shifted the focus to a higher level of detail in the representation of key components of hydrogen conversion, namely the electrolyser and stationary fuel cell.

In standard PyPSA models, these components are represented using "link" elements, which assume a fixed conversion efficiency. However, actual electrolysers and fuel cells exhibit non-linear efficiency curves that vary with the input power. Furthermore, their operation typically excludes very low partial load conditions (usually below 5 %–20 % of rated power), where it is more efficient to shut down the unit rather than operate inefficiently [43].

Capturing these features required the introduction of binary variables, thus moving from the default LP formulation of PyPSA to a MILP framework. This is enabled by integrating the PyPSA network into a Linopy model, which allows retrieval of variables and the addition of custom constraints.

To represent the variable efficiency behaviour, a PWA linear approximation is developed, as described in Ref. [19]. Specifically, for the electrolyser, a five-segment PWA linearization is adopted, based on a MW-scale system already applied in Ref. [42], while fuel cell performance curve and modulation range are assumed as in Ref. [19].

A complete description of the adapted modelling approach, including the mathematical formulation and set of constraints, is provided in Section S1 of the Supplementary Material.

2.3.2. Modelling implementation of hydrogen leakages

Another novelty introduced in this study is the implementation within the model of both intentional and unintentional hydrogen leakages across the value chain.

Leakage rates currently reported in the literature are subject to significant uncertainty, mainly due to the scarcity of experimental measurements, which would require high-precision sensors that are not yet commercially available. To address this uncertainty, each simulation was run twice, assuming the lowest and highest emission rates reported in Ref. [15]. Accordingly, the main results are presented as ranges or as average values with associated error bands.

The technical implementation of the leakage modelling into the system structure is detailed in the Appendix B section.

The assumed leakage rates for each component of the hydrogen value chain are summarised in Table 1.

2.4. Indicators

The optimisation results primarily provide the optimal sizing of system components and the optimal dispatch of energy flows across all timesteps. Based on these outputs, a set of Key Performance Indicators (KPIs) is derived to assess the system's behaviour and its competitiveness from both techno-economic and environmental perspectives.

2.4.1. Techno-economic indicators

- Electrolysis renewable share (RS_{EL}, in %), reflecting the amount of renewable power input over the total electricity supplied to the electrolyser.

$$RS_{EL} = \frac{\sum_{t}^{T} \left(P_{EL,RES}(t) \cdot \Delta t\right)}{\sum_{t}^{T} \left(\left(P_{EL,RES}(t) + P_{EL,grid}(t)\right) \cdot \Delta t\right)} \tag{8}$$

where $P_{EL,RES}(t)$ and $P_{EL,grid}(t)$ represent the power supplied to the electrolyser at time step *t* by the renewable block (PV, wind farm and BESS) and the electric grid, respectively. These values are integrated over the entire time horizon $T = 8760$ hours to compute the total energy supplied from each source.

- Levelised Cost of Hydrogen ($LCOH$, in €/kg$_{H2}$). It is typically calculated as a key indicator to assess the cost-effectiveness and economic competitiveness of hydrogen systems, enabling straightforward comparisons across different configurations. However, in a multi-vector system such as the one modelled here, applying the conventional formulation would lead to a significant overestimation. This is because the full cost contributions from power generation assets, sized to meet both electricity and hydrogen demands, would be entirely attributed to hydrogen production. To address this, an adjusted formulation is proposed, wherein the cost contributions from renewable generators and the electric grid are weighted according to the share of energy actually supplied to the electrolyser relative to their total production. Additionally, the total leaked hydrogen amount $M_{H_{2,leaked}}$ is subtracted from the produced quantity $M_{H_{2,produced}}$ to account economically for emission losses.

$$LCOH = \frac{NPC_{RES} \cdot ES_{RES} + NPC_{grid} \cdot ES_{grid} + NPC_{H2,value\_chain}}{M_{H_{2,produced}} - M_{H_{2,leaked}}} \tag{9}$$

where NPC_{RES} is the aggregated term for the renewable block (PV, wind farm, and BESS), which includes annualised costs and the revenues from selling curtailed electricity under the FIT scheme (counted as negative costs), as explained in Section 2.3. NPC_{grid} accounts for the electricity purchases from the grid, while $NPC_{H2,value\_chain}$ encompasses all expenses associated with the electrolyser, LPST and HPST, compressor and HRS. The costs associated with the fuel cell are excluded from this formulation, as this component is linked to electricity supply and not to hydrogen production. The term ES_i denotes the electrolysis share of generator *i* (with i = RES, grid) and is calculated as follows:

$$ES_{RES} = \frac{E_{EL,RES}}{E_{RES}} = \frac{\sum_{t}^{T} \left(P_{EL,RES}(t) \cdot \Delta t\right)}{\sum_{t}^{T} \left(P_{RES}(t) \cdot \Delta t\right)} \tag{10}$$

$$ES_{grid} = \frac{E_{EL,grid}}{E_{grid}} = \frac{\sum_{t}^{T} \left(P_{EL,grid}(t) \cdot \Delta t\right)}{\sum_{t}^{T} \left(P_{grid}(t) \cdot \Delta t\right)} \tag{11}$$

where $P_{RES}(t)$ and $P_{grid}(t)$ represent the total power output at time step t from the renewable block and the grid, respectively. These quantities are integrated over the full time horizon to compute E_i, i.e., the total yearly energy supplied by generator i.

- Aggregated Levelised Cost of Energy (*LCOE*, in €/kWh). To provide a unified techno-economic indicator for the entire hydrogen valley system, an aggregated Levelised Cost of Energy (LCOE) is introduced, similarly to what Moccia calculated as Levelised Cost of System (LCOS) in Ref. [45]. This metric captures the overall cost of supplying both electricity and hydrogen. The LCOE is defined as:

$$LCOE = \frac{NPC_{tot}}{E_{electricity} + \left(E_{H_{2,produced}} - E_{H_{2,leaked}}\right)} \tag{12}$$

where $E_{electricity}$ is the total electric energy supplied to the load, while $E_{H_{2,produced}}$ and $E_{H_{2,leaked}}$ represent the energetic content of produced and leaked hydrogen based on the Lower Heating Value (LHV).

- Electric load coverage (ELC_i, in %). To evaluate how the electric load is distributed among different sources, the electric load coverage *ELC* is calculated for each generator or group i, according to the following formulation:

$$ELC_i = \frac{E_{electricity,i}}{E_{electricity}} \tag{13}$$

where $E_{electricity,i}$ is the amount of electricity supplied to the load by generator or group i, while the subscript i refers to the renewable block (PV, renewable and BESS), the electric grid, and the fuel cell.

2.4.2. Environmental indicators

- Hydrogen Carbon Intensity (CI_{H2}, in $kg_{CO2\text{-}eq}/kg_{H2}$). The environmental impact in terms of CO_2-equivalent emissions associated with the consumption of grid electricity is estimated by assuming the average carbon intensity of the Cretan electric grid CI_{grid}, equal to 650 $g_{CO2\text{-}eq}$/kWh [29], which is significantly higher than the national average for mainland Greece (206 $g_{CO2\text{-}eq}$/kWh [46]). Consequently, the monitoring of carbon emissions associated with hydrogen production via grid-connected electrolysis becomes particularly important, especially in contexts where the emission intensity of the grid remains high. Accordingly, the carbon intensity of the produced hydrogen is defined as the ratio between the total CO_2-equivalent emissions and the net amount of available hydrogen, calculated as the total hydrogen production minus the amount lost through emissions:

$$CI_{H2} = \frac{CI_{grid} \cdot E_{grid} \cdot ES_{grid}}{M_{H_{2,produced}} - M_{H2,leaked}} \tag{14}$$

- Hydrogen Emissions (*HE*, in t). Since the environmental impact of a hydrogen valley is not limited to CO_2-eq emissions associated with grid electricity use, but also includes climate-altering hydrogen emissions, this aspect is assessed by estimating the potential range of hydrogen released across the system. Hydrogen emissions are calculated based on the hydrogen mass flow rate and the leakage rates associated with the electrolyser, compressor, HRS and fuel cell. For the two storage tanks, emissions are evaluated as standing losses at each timestep, and thus depending on the Level of Hydrogen (LOH) stored.

The total hydrogen emissions *HE* are calculated as:

$$HE = \sum_{t}^{T} \left(\sum_{i} \left(LR_i \cdot \dot{m}_{H2,i}(t)\right) + \sum_{j} \left(LR_j \cdot LOH_j(t)\right) \right) \cdot \Delta t \tag{15}$$

where $\dot{m}_{H2,i}(t)$ is the hydrogen mass flow rate processed by component i (with i = electrolyser, compressor, HRS, fuel cell) at timestep t, LR_i is the leakage rate associated with component i, $LOH_j(t)$ is the level of hydrogen stored in tank j at timestep t, and LR_j is the leakage rate per hour for storage tank j at timestep t, with j referring to LPST and HPST. Total emissions are computed by integrating the hourly losses through the full time horizon $T = 8760$ hours.

- Relative Hydrogen Loss (*HE*, in %). Defined as the ratio of hydrogen losses due to leakage across the entire value chain ($M_{H2,leaked}$) over the total hydrogen produced ($M_{H2,produced}$):

$$RHL = \frac{M_{H2,leaked}}{M_{H2,produced}} \tag{16}$$

The detailed methodology used to calculate $M_{H2,leaked}$ is provided in the Appendix section.

2.5. Scenarios

The optimisation is performed based on a cost minimisation objective, as shown in Eq. (1), with additional environmental constraints incorporated to evaluate the performance of the hydrogen valley under various conditions.

Different scenarios are investigated:

- First, a baseline scenario without CO_2 constraints is simulated to determine the optimal economic configuration. Assuming therefore no limitations on greenhouse gas emissions, it serves as a benchmark for assessing system performance in the absence of environmental constraints. Average values of hydrogen leakage rates are assumed.
- The resulting grid-related CO_2-eq emissions are then used as a reference for a sensitivity analysis assuming CO_2-eq-constrained scenarios, in which progressively stricter emission limits are applied, reducing allowable emissions in 10 % increments, up to a fully decarbonised scenario. Each sensitivity analysis scenario is run twice with the upper and lower limits of the hydrogen emission estimates to assess the impact of this variability on the KPIs.

2.6. Demand estimation and input data

To exploit the cross-sectoral potential of hydrogen valleys, the modelled system is designed to serve different types of energy demand, acting as a flexible hub connecting different end users. Hydrogen is supplied to a fleet of three fuel cell-powered touristic buses and a fuel cell-powered passenger ship (Section 2.6.1). In addition, the system includes an electricity demand profile associated with cold ironing operations for large merchant ships docked at port (Section 2.6.2). These applications reflect hydrogen's growing role as a clean energy carrier in the transport and maritime sectors.

2.6.1. Hydrogen demand

The bus fleet is composed of three coaches, each covering a daily mission of approximately 700 km. This results in one refuelling per bus per day, with a hydrogen consumption of about 50 kg, assuming a tank

Table 2
Assumptions for H_2 demand estimations.

Parameter	Value
Bus fleet	
Fleet size	3 coaches
Operating period	Full year
Tank capacity (per coach)	60 kg_{H2}
Specific consumption (per coach)	0.07 kg_{H2}/km
Daily mission (per coach)	700 km
Trips per day	1
Refuelling frequency	1 per day per coach
Total H_2 demand	150 kg_{H2}/day
Passenger ship	
Fleet size	1 ship
Operating period	From 1 May to 31 October
Specific consumption	36 kg_{H2}/h
Trip duration	2 h
Trips per day	2
Refuelling frequency	2 per day
Total H_2 demand	144 kg_{H2}/day

capacity of 60 kg of hydrogen per coach and a specific consumption of 7 kg H_2 per 100 km [47].

Regarding the ship load, a demand profile is derived from a previous study conducted as part of the CRAVE-H_2 project [48]. The scenario assumes the replacement of a 0.6 MW diesel engine with a fuel cell system operating at 50 % efficiency, leading to an hourly hydrogen consumption of approximately 36 kg. Additional details regarding the trips and refuelling scheduling are provided in Table 2, while Fig. 2 illustrates the hourly refuelling profile for a representative day during the tourist season.

2.6.2. Electricity demand

The model incorporates an electricity demand profile representing cold ironing operations for large ships docking at the port. It is assumed that the hydrogen valley supplies electricity to the port authority, with the renewable supply either supported by a hybrid storage system (fuel cell and BESS) or supplemented by grid electricity during renewable shortfalls, as shown in Fig. 1.

Consistent with the modelling of the passenger ship's hydrogen demand, the cold ironing demand profile is developed using data provided by CRAVE-H2 project partners and detailed in Ref. [47]. Specifically, monthly energy requirements are estimated using methodologies established in the literature [14,49], and based on publicly available data from the Heraklion Port Authority. From this baseline, a weekly electricity demand profile is constructed and normalized to reflect the estimated monthly energy consumption, as illustrated in Fig. 3.

2.6.3. Input data

This section presents all the exogenous input data used in the model, summarising data provided by the CRAVE-H_2 project consortium and assumptions derived from the literature. All the data are listed in Table 3.

3. Results

3.1. Base scenario

First, the unconstrained CO_2-eq scenario, referred to as the base scenario, is examined with the objective of identifying the purely techno-economic optimal configuration of the plant.

Given the wide uncertainty in hydrogen leakage rates reported in the literature, the base scenarios adopt average values between the upper

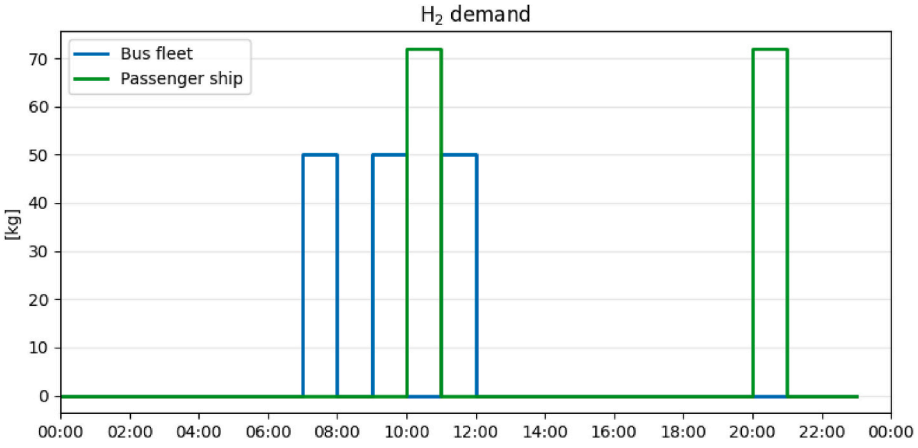

Fig. 2. Daily hydrogen refuelling demand during touristic season (from May 1 to October 31).

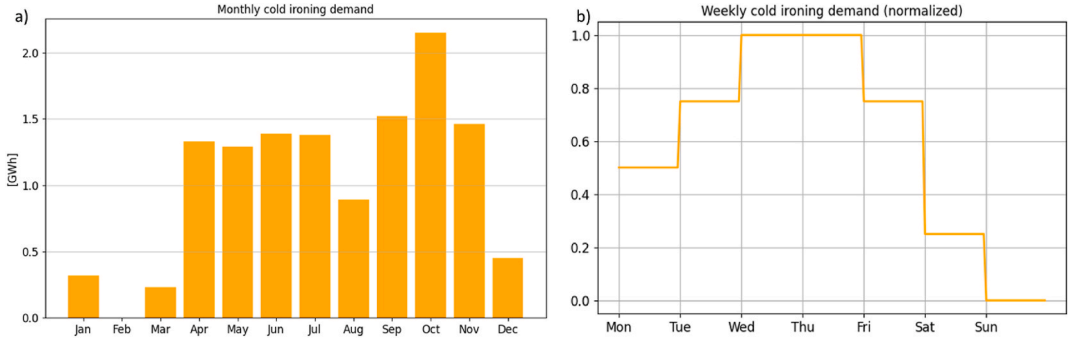

Fig. 3. Cold ironing electrical demand, a) Monthly demand estimates [48], b) normalized weekly profile.

Table 3
Input data used in the model.

	Value	Ref.
Photovoltaic		
Power availability	2019 capacity factor timeseries in valley's site (Atherinolakkos)	[50]
CAPEX	650 €/kW	[51]
OPEX (annual)	2 % of CAPEX	[52]
FIT selling price	63 €/MWh	[41]
Lifetime	Project lifetime	
Wind farm		
Availability	2019 capacity factor timeseries in valley's site (Atherinolakkos)	[53]
CAPEX	1120 €/kW	[51]
OPEX (annual)	3 % of CAPEX	[42]
FIT selling price	72 €/MWh	[41]
Lifetime	Project lifetime	
Electric grid		
Purchase price	2019 Greece retail electricity time series (0.06382 €/kWh average)[a] + 0.001 €/kWh[b]	[55]
Connection cost	200 €/kW	[56]
Carbon intensity	650 $g_{CO2\text{-}eq}$/kWh	[29]
Battery storage		
CAPEX (module + BOP)	306 €/kW	[57]
OPEX (annual)	2 % of CAPEX	[58]
Replacement cost (module)	50 % of CAPEX	[58]
Lifetime of module	10 years	[58]
Lifetime of BOP	Project lifetime	
Charging efficiency	95 %	[58]
Discharging efficiency	95 %	[58]
Min. SOC	20 %	[58]
Max. SOC	100 %	[58]
C-rate	1C	
Electrolyser		
CAPEX (stack + BOP)	1188 €/kW	[59]
OPEX (annual)	3 % of CAPEX	[42]
Efficiency	PWA of efficiency curve	[42]
Modulation range	5–100 % (of nominal power)	[43]
Replacement cost (stack)	30 % of CAPEX	[60]
Lifetime of stack	65000 h (2 replacements during lifetime)	[61]
Lifetime of BOP	Project lifetime	
Hydrogen compressor		
CAPEX	330 €/kW_{H2} (11000 €/(kg_{H2}/h))	[62]
OPEX (annual)	2 % CAPEX	[63]
Electric consumption (compression from 30 to 350 bar)	1.52 kW_e/kg_{H2}	[64]
Lifetime	Project lifetime	
Fuel cell		
CAPEX	2000 €/kW	[65]
OPEX (annual)	3 % of CAPEX	[66]
Efficiency	PWA of efficiency curve	[19]
Modulation range	5.8–100 % (of nominal power)	[19]
Replacement cost (stack)	46 % of CAPEX	[66]
Stack lifetime	65,000 h (2 replacements during lifetime)	[61]
Lifetime of BOP	Project lifetime	
Hydrogen storage tanks		
CAPEX	500 €/kg_{H2} for LPST (type I storage) 1100 €/kg_{H2} for HPST (type III storage)	[67]
OPEX (annual)	2 % of CAPEX	[63]
Min. LOH	20 %	
Max. LOH	100 %	
Operating pressure	30 bar for LPST, 350 bar for HPST	Project data
Lifetime	Project lifetime	
Hydrogen refuelling station		
CAPEX	650 €/kW	Combination of [68] and project data
OPEX	2 % of CAPEX	[68]
Other assumptions		
Project lifetime	20 years	
Discount rate	5 %	

[a] The hourly electricity retail price trend in 2019 is provided in section S2 of the Supplementary Material.
[b] A constant tariff, provided by project partners [54], is added to the hourly wholesale electricity price to account for service charges, dispatching costs, taxes, and other regulatory fees. This adjustment also reflects the higher electricity production costs in Crete compared to mainland Greece.

and lower estimates. The optimal system sizing resulting from this base scenario is presented in Fig. 4 and Table 4.

It is evident that the optimisation process chooses to not invest in storage solutions besides the HPST, which is used to supply the HRS. Therefore, the system strongly depends on the electric grid supply rather than exploiting renewable energy storage options based on the BESS and the LPST, the latter being closely linked to the use of fuel cells.

During the peak hydrogen demand period, which runs from May to October when touristic ferries are in operation, the electrolyser operates at nominal capacity, as can be noted in Fig. 5. In this phase, the electric grid plays a critical role in stabilising the power supply by compensating for the variability of renewable generation. As a result, grid electricity accounts for more than 67 % of the electrolyser's total energy input on a yearly basis. With a renewable share of slightly less than 33 %, the produced hydrogen exhibits a high carbon intensity of just above 27 $kg_{CO2\text{-}eq}$/kg_{H2}. This finding aligns with the IEA's Global Hydrogen Review [1], which states that every 100 $g_{CO2\text{-}eq}$/kWh of electricity results in approximately 5 $kg_{CO2\text{-}eq}$/kg_{H2}. Consequently, when large shares of high-carbon grid electricity are used, as in Crete where the grid intensity approaches 700 $g_{CO2\text{-}eq}$/kWh_e, the carbon footprint of electrolytic hydrogen exceeds that of hydrogen produced from unabated natural gas.

From an economic perspective, the system demonstrates satisfactory competitiveness, yielding an LCOH of 6.47 €/kg_{H2}, a value consistent with findings from other LCOH studies focused on HRSs [69,70]. Additionally, the aggregated LCOE is estimated at 75.54 €/MWh. As discussed in Section 2.4.1, few studies have conducted levelised cost analyses for multi-vector energy systems, which introduces a degree of uncertainty when benchmarking economic performance. Nevertheless, the result aligns with the findings of Moccia [45], who reported LCOE values ranging from 55 to 119 €/MWh, depending on assumptions regarding the integration of renewable and nuclear energy sources in a dual electricity-hydrogen supply configuration.

The main KPIs from the base scenario simulation are summarised in Table 5.

3.2. CO_2-eq-constrained scenarios

When CO_2 emissions caps are imposed, the system configuration undergoes significant changes, particularly as the fully zero-carbon condition is approached. In this scenario, the restriction on the use of grid electricity (due to the associated carbon intensity) drives substantial investments across all storage technologies, as well as in significantly larger renewables capacity. As shown in Fig. 6, reporting average values of hydrogen leakage rates, notable capacity increases are observed in both the PV-BESS and fuel cell-LPST systems. Special attention should be given to the latter, where the fuel cell capacity

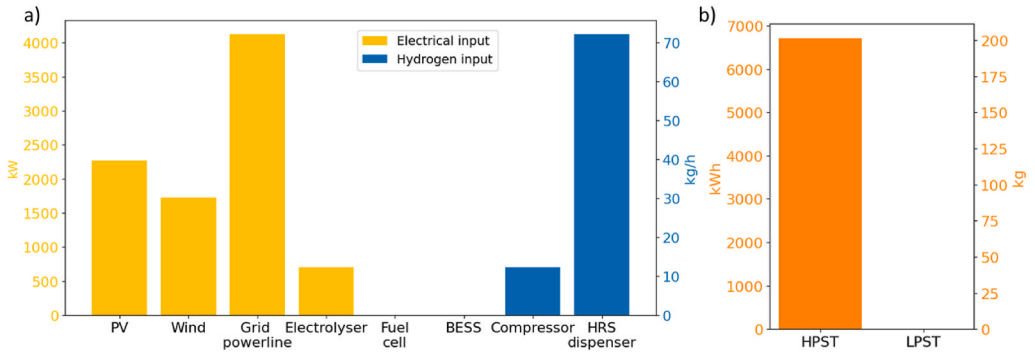

Fig. 4. Optimal sizes in the base scenario assuming average H_2 leakage rate values: a) Capacity referred to input flow; b) Capacity referred to storing size.

Table 4
Optimal components sizes in the base scenario with average H_2 leakage rate values.

Optimal sizes		
Component	Size	Unit of measurement
PV	2283	kW
Wind	1705	kW
Grid connection to electrolysis	702	kW
Grid connection to electric demand bus	3424	kW
Electrolyser	702	kW
Fuel cell	0	kW
Battery	0	kWh
Compressor	12	kg_{H2}/h
HRS dispenser	72	kg_{H2}/h
LPST	0	kg_{H2}
HPST	201	kg_{H2}

exceeds that of the electrolyser, and the optimal sizing of the LPST reaches over 8000 kg of hydrogen.

From the generation side, the model reveals a shift in investment preference toward PV systems over wind turbines as BESS capacity increases. This trend suggests that the optimisation process leverages the cost advantages of solar energy, which, when coupled with sufficient storage, becomes more economically attractive than wind power under constrained emission scenarios.

It should be noted that different hydrogen leakage rate estimates can influence the optimal sizing of system components. Higher leakage rates may lead to slight oversizing of certain components to compensate for increased hydrogen losses and maintain supply reliability. However, this impact is generally limited, with most components exhibiting size variations of less than 6 % between the lowest and highest hydrogen leakage scenarios.

The imposition of CO_2-eq emission caps has a significant impact on the system's total costs, as illustrated by the LCOH and LCOE trends in Figs. 7 and 8, respectively. These figures highlight the contribution of each system component to the total cost, along with the revenues from excess renewable energy valorised through the FIT scheme, which are represented as negative costs reducing the overall value. To better capture the variability introduced by hydrogen emissions, the results are shown as average values between scenarios with the lowest and highest leakage rates, with error bands representing the full uncertainty range.

Competitive LCOH values, ranging from 5.36 to 8.21 €/kg_{H2}, are achieved in all scenarios except for the fully decarbonised one, where the average cost sharply increases to around 15 €/kg_{H2}. This is mainly due to the substantial investment required for the LPST, which is closely tied to the operation of the fuel cell and significantly impacts overall cost-effectiveness.

As the system transitions toward zero-carbon configurations with increasing renewable capacity, the revenues from excess electricity, represented by negative cost contributions, play an important role in mitigating the rise in investment costs. In this context, the FIT applicable to non-interconnected islands such as Crete [41] becomes a key factor. The most favourable outcome is observed in the 60 % CO_2 cap scenario, with LCOH values of 5.36 and 5.73 €/kg_{H2} for the lowest and highest hydrogen leakage assumptions, respectively. Nevertheless, FIT revenues alone are insufficient to keep the LCOH below the 10 €/kg_{H2} threshold in the fully decarbonised scenario, highlighting the need for additional support mechanisms and related incentives.

As observed in Fig. 7, the total LCOH trend (including excess electricity revenues) is not strictly monotonic: more stringent CO_2-eq constraints lead to slight cost reductions before rising again in the fully decarbonised scenario. This behaviour is driven by two main factors.

Table 5
KPIs from the base scenario simulation (assuming average H_2 leakage rate values).

Indicator	Result
RS_{EL}	32.41 %
CI_{H_2}	27.1 $kg_{CO2\text{-}eq}/kg_{H2}$
LCOH	6.47 €/kg_{H2}
LCOE	75.54 €/MWh

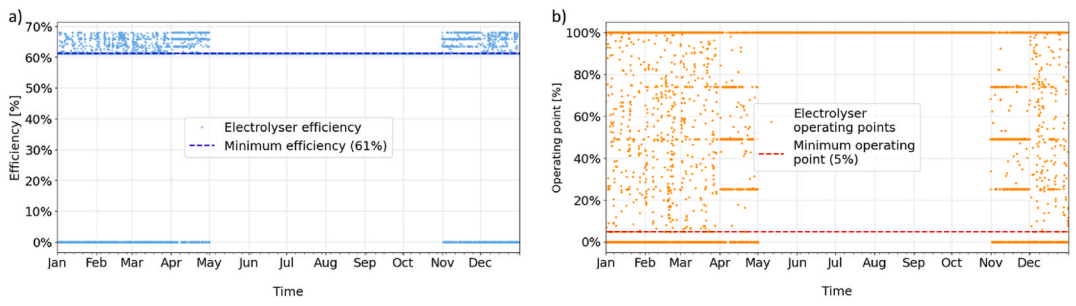

Fig. 5. Efficiency (a) and operating point (b) of the electrolyser across the year in the base scenario.

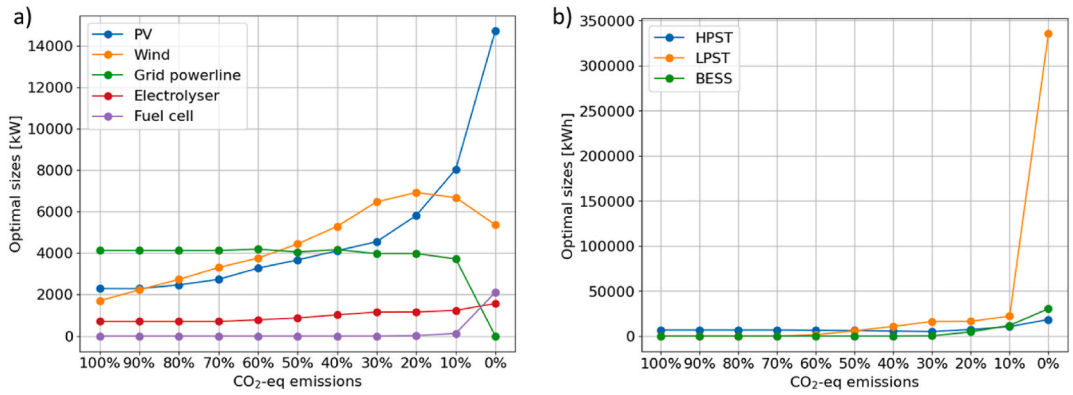

Fig. 6. Optimal sizes in CO_2-eq emissions cap sensitivity analysis assuming average H_2 leakage rate values: a) Process flow components; b) Storage components.

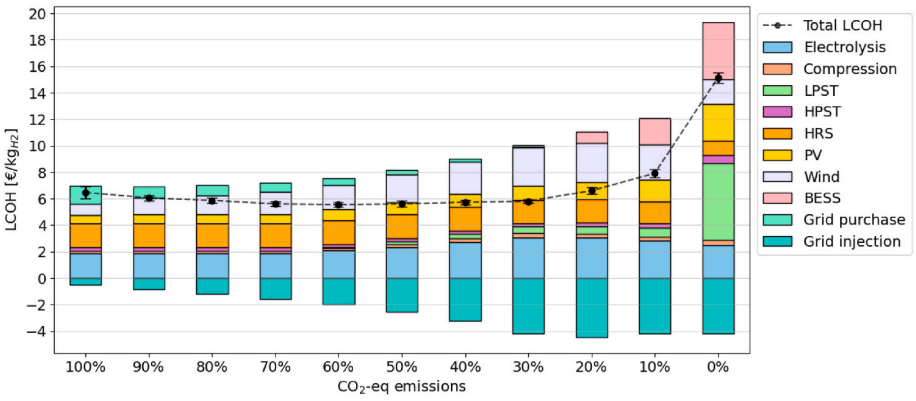

Fig. 7. LCOH across the various CO_2-eq emissions-constrained scenarios, assuming average H_2 leakage rate values with error bands reflecting lowest and highest estimates.

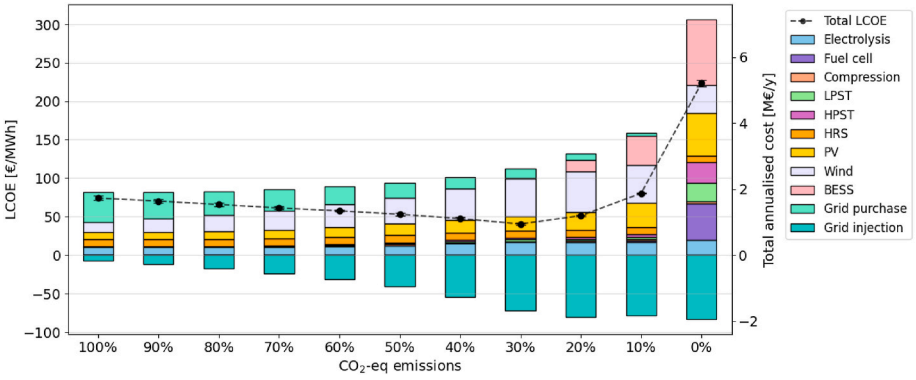

Fig. 8. Aggregated LCOE for the techno-economic assessment of the entire system with increasing CO_2-eq emission caps, assuming average H_2 leakage rate values with error bands reflecting lowest and highest estimates.

First, the multi-vector structure of the demand supplied by the valley leads the optimisation process to minimise the total system cost across all energy carriers, rather than focusing on each vector individually. As a result, in the unconstrained scenario, the model may prioritise the cheapest overall electricity supply strategy, even if it results in slightly higher hydrogen production costs. Second, the revenues from excess renewable energy, calculated post-optimisation, reveal cost-optimal configurations at intermediate CO_2-eq constraint levels, resulting in a balanced mix of grid electricity and renewable capacity. Without accounting for these revenues, the LCOH would exhibit a more predictable, monotonic increase. This effect is more clearly illustrated in Fig. 8, which shows the evolution of the aggregated LCOE. When focusing only on the positive cost contributions (i.e. excluding FIT revenues), a consistent upward trend emerges. Notably, the lowest aggregated LCOE occurs under stricter CO_2-eq caps than the LCOH minimum, with the most cost-effective configuration reached at a 30 % CO_2-eq emissions level, reflecting the key role of the excess renewable energy sales when increasing PV, wind and BESS capacities.

The variability introduced by hydrogen emissions is less pronounced than in the LCOH results, as indicated by the narrower error bands. This result is expected, as the impact of hydrogen losses is mitigated when assessing the feasibility of the overall system costs, which also includes electricity supply.

Shifting the focus from hydrogen to electricity demand, it is worth

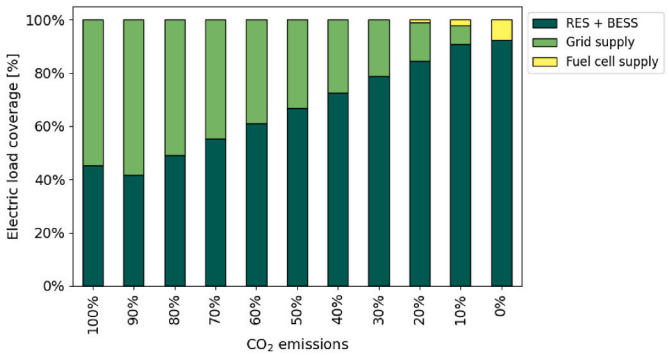

Fig. 9. Electric load coverage assuming average H_2 leakage rate values with increasing CO_2-eq emission caps.

examining how the electric load is met by the various system components. Fig. 9 illustrates the share of electricity supplied by renewable generators and battery, the electric grid, and the fuel cell, under the assumption of the average hydrogen leakage rate. As shown, the large share of grid electricity in the base scenario is gradually replaced by growing contributions from renewables and BESS as the CO_2-eq emissions cap tightens. The fuel cell, by contrast, contributes marginally in the 20 %, 10 % and fully decarbonised scenarios. This limited role reflects its poor cost-effectiveness, primarily due to the low round-trip efficiency of converting electricity into hydrogen and back into electricity.

3.3. Hydrogen emissions

For a comprehensive environmental assessment of the modelled system, hydrogen leakages must also be considered. Fig. 10 presents the total hydrogen emissions across the sensitivity scenarios, both in absolute terms and as a percentage of total hydrogen produced.

The amount of leaked hydrogen remains relatively constant across the scenarios, particularly in relative terms, except for the fully decarbonised scenario where a marked increase is observed. This spike is primarily due to the substantial expansion of the LPST, whose leakage is directly proportional to the quantity of stored hydrogen.

The wide variability observed in the emission ranges, as discussed in Section 2.4, is mainly caused by the limited availability of experimental data in the literature. It can be noted that the electrolyser is the dominant source of this uncertainty, largely due to the potential inclusion of purging operations [22]. These, along with venting, are classified as intentional emissions and differ from other leakage events, which are typically unintentional, such as permeation losses in storage systems. A more detailed breakdown of emission losses along the hydrogen value chain is provided in Fig. 11, referring to an average emissions estimate under the fully decarbonised scenario.

It is important to emphasise that the quantification of hydrogen emissions presented in this work should not be interpreted as an exact prediction of leakage levels, but rather as an indication of the potential scale of losses under different conditions, ranging from favourable to unfavourable. The intention is to encourage stakeholders to proactively consider investments in leakage monitoring and prevention systems, such as the deployment of high-precision sensors along the hydrogen value chain. In addition, careful handling of electrolysers is crucial, in particular acting on purging events, which are often cited in the literature as being mainly responsible for hydrogen leakage, by reducing them and recombining the expelled hydrogen. With proper mitigation strategies, total hydrogen emissions can be kept below 2 % of total production even in a zero-carbon scenario, as shown in Fig. 10.

4. Conclusions

A techno-economic optimisation model, developed within a MILP

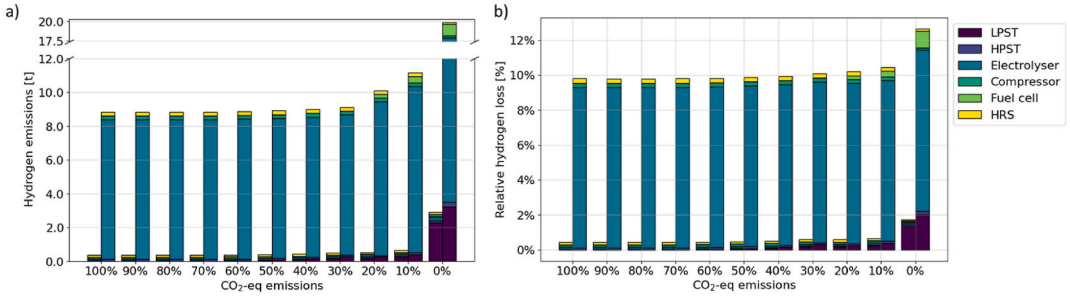

Fig. 10. Lowest and highest possible hydrogen emissions amounts in the CO_2-eq emission caps sensitivity analysis. a) Absolute quantity; b) Relative quantity to total production.

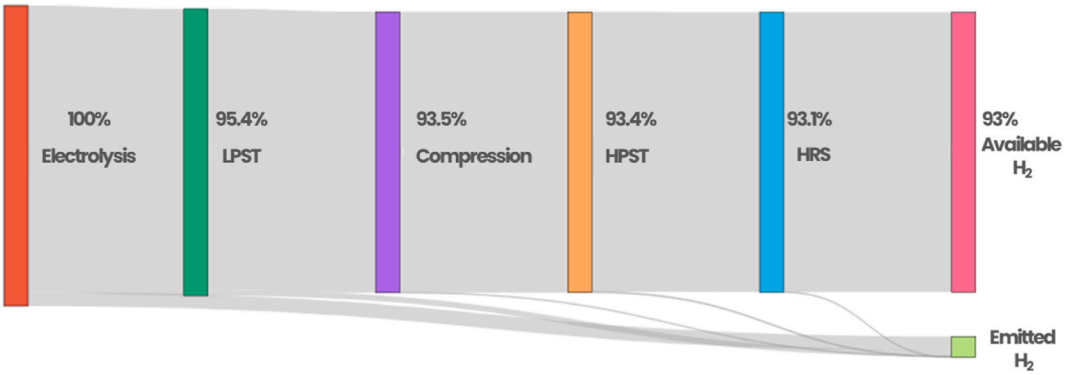

Fig. 11. Hydrogen losses across the value chain in fully decarbonised scenario assuming average values of leakage rates. Losses in the fuel cell are excluded, as they relate to electricity use rather than hydrogen demand.

framework, was designed to assess the performance of a hydrogen valley currently under construction in southeastern Crete, supplying both hydrogen and electricity for tourism-oriented mobility and cold ironing of large ships at berth. To enhance the technical realism of key components, a customised modelling configuration for electrolysers and fuel cells was implemented in PyPSA, combined with Linopy for greater flexibility. In particular, this novel approach enables the representation of a continuous PWA approximation of the non-linear efficiency curves, while also accounting for modulation limits imposed by minimum operating thresholds, a level of detail not typically supported in default PyPSA implementations.

To ensure a more comprehensive evaluation, the model also incorporates estimates of hydrogen leakage rates as reported in the literature, providing the basis for further GWP calculations (through the quantification of potential atmospheric hydrogen release) and the economic consequences of losing a non-negligible share of the produced hydrogen along the value chain.

Finally, the sale of excess renewable energy is calculated post-optimisation to avoid diverting the capacity planning focus away from hydrogen production. This is done under the assumption of a favourable FIT scheme applicable to RES systems in non-interconnected areas of Greece.

The system was tested under a range of operational scenarios, beginning with a baseline case without CO_2-eq emission constraints, which served as a reference point for a sensitivity analysis. This analysis progressively introduced tighter CO_2-eq emission caps, ultimately leading to a fully decarbonised configuration.

The main conclusions drawn from this modelling effort can be summarised as follows:

- When revenues from excess renewable energy are excluded, the system favours grid-dependent configurations to minimise costs. Although this approach yields competitive techno-economic indicators, it does not meet decarbonisation standards. In the unconstrained scenario, hydrogen production results in a carbon intensity of approximately 27 $kgCO_2$-eq/kgH_2, exceeding the 10–12 $kgCO_2$-eq/kgH_2 benchmark for natural gas-based hydrogen.
- Imposing emission caps reshapes the system layout, with fully decarbonised scenarios requiring high investments in renewable and storage capacity. These changes significantly raise costs, particularly due to fuel cell inefficiencies. Nevertheless, favourable FIT schemes available in non-interconnected regions like Crete help offset costs, maintaining LCOH between 5.36 and 8.21 €/kgH_2 across most scenarios. In the fully decarbonised case, LCOH rises to around 15 €/kgH_2 (average between leakage scenarios), underlining the need for complementary incentives.
- The inclusion of FIT revenues substantially improves system performance, both economically and environmentally. This compensation mechanism incentivises larger renewable installations and shifts the cost-optimal configuration (in terms of LCOE) from the unconstrained case to a configuration emitting 70 % less CO_2-eq emissions.
- Fuel cells prove to be a useful backup in off-grid scenarios, complementing BESS to address renewable shortages. However, due to their low round-trip efficiency, their viability is closely linked to a market environment characterised by targeted incentives for feeding electricity into the grid, which are currently absent in Greek legislation, and considerable volatility in electricity prices. Future work could explore appropriate FIT levels to support these applications.
- Hydrogen emissions, particularly those from purging and venting, should be taken into account in both environmental and cost assessments. Fully decarbonised layouts show slightly higher losses (up to 12.28 % in worst-case scenarios, compared to 9.8 % in unconstrained scenarios) due to storage oversizing. These results highlight the importance of investing in hydrogen emission monitoring systems and optimising electrolyser operation. With mitigation strategies, leak rates could realistically remain below 2 %, even in configurations with high renewable energy content.

Limitations of this study include its zero-dimensional spatial resolution, which prevents the assessment of hydrogen transport costs. While these are expected to be minimal due to the limited geographical scope of the hydrogen valley in its initial phase, their exclusion remains a modelling simplification. Future work will expand the spatial dimension to a regional scale to assess how the geographic distribution of value chain elements affects both performance and cost.

Moreover, in the absence of explicit temporal/conditional restrictions in the referenced FIT documentation, all curtailed RES energy is treated as FIT-eligible, representing a best-case revenue estimate. Future work should test alternative eligibility rules (e.g., time-of-day filters) and, if needed, conduct a system-wide market analysis for Crete to capture congestion-related constraints. This, in turn, would provide a basis for examining how hydrogen valleys interact with local networks, particularly their potential contribution to ancillary services and balancing markets.

CRediT authorship contribution statement

Vincenzo Romano: Writing – original draft, Visualization, Software, Resources, Methodology, Investigation, Formal analysis, Data curation, Conceptualization. **Paolo Marocco:** Writing – review & editing, Visualization, Validation, Supervision, Project administration, Conceptualization. **Marta Gandiglio:** Writing – review & editing, Visualization, Validation, Supervision, Project administration, Conceptualization. **Massimo Santarelli:** Writing – review & editing, Supervision, Funding acquisition.

Declaration of generative AI and AI-assisted technologies in the writing process

During the preparation of this work the authors used ChatGPT 4.0 in order to improve the quality of language and readability. After using this tool/service, the authors reviewed and edited the content as needed and take full responsibility for the content of the publication.

Declaration of competing interest

The authors declare that they have no known competing financial interests or personal relationships that could have appeared to influence the work reported in this paper.

Acknowledgements

The project is supported by the Clean Hydrogen Partnership and its members (Project Crete Aegean H2 Valley, Grant Agreement No. 101112169).

Appendix A. Supplementary data

Supplementary data to this article can be found online at https://doi.org/10.1016/j.ijhydene.2025.152172.

Appendix B

Modelling implementation of hydrogen leakages

Hydrogen emissions, both intentional and unintentional, are modelled by converting PyPSA standard "links" into "multi-links", allowing connections to multiple input and output buses.

In this framework, the links representing the hydrogen flow components are modified to include a bifurcation that directs the leakage flow to a dedicated emission bus, where a Negative Dispatch Generator (NDG) collects the total leaked hydrogen. Specifically, each adapted link is connected to two output nodes, with the efficiency parameters defined as follows:

$$\dot{m}_{j,out}(t) = \left(\varepsilon_j - LR_j\right) \cdot \dot{m}_{j,in}\ (t) \tag{B1}$$

$$\dot{m}_{j,leaked}(t) = LR_j \cdot \dot{m}_{j,in}\ (t) \tag{B2}$$

$$M_{H2,j,leaked} = \sum_{t}^{T} \dot{m}_{j,leaked}(t) \cdot \Delta t \tag{B3}$$

where $\dot{m}_{j,out}$, $\dot{m}_{j,in}$, $\dot{m}_{j,leaked}$ represent the output, input, and leaked hydrogen flow rates, respectively, and ε_j is the actual conversion efficiency while LR_j denotes the leakage rate. All quantities are defined for each component j at every timestep t, where j refers to the electrolyser, compressor, HRS dispenser and fuel cell. The total leaked hydrogen mass $M_{H2,j,leaked}$ is obtained by integrating the leakage flow values over the full simulation interval $T = 8760$ hours.

It is important to note that $\dot{m}_{in}$ for the electrolyser actually corresponds to its hydrogen output flow (as the actual input is electricity), which is then reduced to account for emission losses downstream in the system. Moreover, ε_j is set to 1 for the electrolyser as the efficiency is modelled as described in Section S1.

For the two hydrogen storage tanks (LPST and HPST), leakage due to permeation is modelled through the "standing_loss" parameter of PyPSA's "StorageUnit" component. The total hydrogen emissions from storage are calculated as (with j = LPST and HPST):

$$M_{H2,leaked,storage} = \sum_{t}^{T} \left(\sum_{j} \left(LOH_j(t-1) \cdot E_j \cdot LR_j\right) \cdot \Delta t \right) \tag{B4}$$

with LOH_j is the hourly level of hydrogen in tank j with rated capacity E_j. The hourly loss in timestep t is calculated based on the LOH in previous timestep, and it is integrated over the full time horizon $T = 8760$ hours to obtain the total leaked hydrogen mass.

In principle, venting losses during start-up and shut-down could be modelled dynamically using the electrolyser's on/off status. However, given that these losses are very small (approximately 0.06–0.5 % of total production), they have been represented as a continuous loss proportional to the produced hydrogen flow, which is a reasonable simplification in view of the trade-off between model detail and computational burden.

Nearly all hydrogen emissions in electrolysis stem from purging, which occurs continuously while the electrolyser is operating. Moreover, the upper bound of 9.2 % is reported as a conservative value and is unlikely in practice, while purging rates around 3–4 % are considered more realistic [44].

Acronyms

BESS	Battery Energy Storage System
BOP	Balance of Plant
CAPEX	Capital Expenditure
FIT	Feed-in Tariff
GWP	Global Warming Potential
HESS	Hydrogen Energy Storage System
HRS	Hydrogen Refuelling Station
KPI	Key Performance Indicator
LCOE	Levelised Cost of Energy
LCOH	Levelised Cost of Hydrogen
LHV	Lower Heating Value
LOH	Level of Hydrogen
LP	Linear Programming
MILP	Mixed-Integer Linear Programming
MINLP	Mixed-Integer Non-Linear Programming
NDG	Negative Dispatch Generator
O&M	Operation and Maintenance
OPEX	Operational Expenditure
PV	Photovoltaic
PWA	Piecewise Affine
RES	Renewable Energy Sources
SOC	State of Charge

References

[1] International Energy Agency. Global hydrogen review 2024. www.iea.org; 2024.

[2] McKinsey & Company. Hydrogen insights 2023: the state of the global hydrogen economy, with a deep dive into renewable hydrogen cost evolution. www.hydrogencouncil.com; 2023.

[3] Clean hydrogen partnership, hydrogen valleys, (n.d.). https://www.clean-hydrogen.europa.eu/get-involved/hydrogen-valleys_en (accessed May 27, 2025).
[4] European Commission, Exploring hydrogen's potential in island communities: webinar highlights, (n.d.). https://clean-energy-islands.ec.europa.eu/news/exploring-hydrogens-potential-island-communities-webinar-highlights#:~:text=Renewable%20hydrogen%20stands%20as%20a%20crucial%20energy,security%20and%20independence%20from%20fossil%20fuel%20imports. (accessed May 29, 2025).
[5] Bampaou M, Panopoulos KD. An overview of hydrogen valleys: current status, challenges and their role in increased renewable energy penetration. Renew Sustain Energy Rev 2025;207:114923. https://doi.org/10.1016/J.RSER.2024.114923.
[6] Clean hydrogen partnership, hydrogen valleys map, (n.d.). https://h2v.eu/hydrogen-valleys (accessed May 29, 2025).
[7] Fachrizal R, Shepero M, van der Meer D, Munkhammar J, Widén J. Smart charging of electric vehicles considering photovoltaic power production and electricity consumption: a review. ETransportation 2020;4:100056. https://doi.org/10.1016/J.ETRAN.2020.100056.
[8] Mendler F, Voglstätter C, Müller N, Smolinka T, Holst M, Hebling C, Koch B. A newly developed spatially resolved modelling framework for hydrogen valleys: methodology and functionality. Adv Appl Energy 2025;17. https://doi.org/10.1016/j.adapen.2025.100207.
[9] Rosén S, Göransson L, Taljegård M, Lehtveer M. Modeling of a "Hydrogen Valley" to investigate the impact of a regional pipeline for hydrogen supply. Front Energy Res 2024;12. https://doi.org/10.3389/fenrg.2024.1420224.
[10] Guichard J, Rawlinson-Smith R, Greaves D. Optimization of reversible solid oxide cell system capacity combined with an offshore wind farm for hydrogen production and energy storage using the PyPSA power system modelling tool. IET Renew Power Gener 2024. https://doi.org/10.1049/rpg2.13134.
[11] Dadkhah A, Bozalakov D, De Kooning JDM, Vandevelde L. On the optimal planning of a hydrogen refuelling station participating in the electricity and balancing markets. Int J Hydrogen Energy 2021;46:1488–500. https://doi.org/10.1016/j.ijhydene.2020.10.130.
[12] Petrollese M, Concas G, Lonis F, Cocco D. Techno-economic assessment of green hydrogen valley providing multiple end-users. Int J Hydrogen Energy 2022;47:24121–35. https://doi.org/10.1016/j.ijhydene.2022.04.210.
[13] Genovese M, Piraino F, Fragiacomo P. 3E analysis of a virtual hydrogen valley supported by railway-based H2 delivery for multi-transportation service. Renew Sustain Energy Rev 2024;191. https://doi.org/10.1016/j.rser.2023.114070.
[14] Conte F, D'Agostino F, Silvestro F. Rethinking ports as multienergy hubs: managing cold ironing and hydrogen supply/bunkering. IEEE Electrification Magazine 2023;11:43–51. https://doi.org/10.1109/MELE.2022.3232981.
[15] Esquivel-Elizondo S, Hormaza Mejia A, Sun T, Shrestha E, Hamburg SP, Ocko IB. Wide range in estimates of hydrogen emissions from infrastructure. Front Energy Res 2023;11. https://doi.org/10.3389/fenrg.2023.1207208.
[16] Ocko IB, Hamburg SP. Climate consequences of hydrogen emissions. Atmos Chem Phys 2022;22:9349–68. https://doi.org/10.5194/acp-22-9349-2022.
[17] CRAVE-H2, CRAVE-H2 project, (n.d.). https://www.crave-h2.eu/(accessed November 18, 2024).
[18] Brown T, Hörsch J, Schlachtberger D. PyPSA: python for power system analysis. https://doi.org/10.5334/jors.188; 2017.
[19] Marocco P, Ferrero D, Martelli E, Santarelli M, Lanzini A. An MILP approach for the optimal design of renewable battery-hydrogen energy systems for off-grid Insular communities. Energy Convers Manag 2021;245. https://doi.org/10.1016/j.enconman.2021.114564.
[20] Raheli E, Werner Y, Kazempour J. A conic model for electrolyzer scheduling. Comput Chem Eng 2023;179. https://doi.org/10.1016/j.compchemeng.2023.108450.
[21] Hofmann F. Linopy: Linear optimization with n-dimensional labeled variables. J Open Source Softw 2023;8:4823. https://doi.org/10.21105/joss.04823.
[22] Trapani D, Marocco P, Gandiglio M, Santarelli M. Hydrogen leakages across the supply chain: current estimates and future scenarios. Int J Hydrogen Energy 2025;145:1084–95. https://doi.org/10.1016/J.IJHYDENE.2025.06.103.
[23] Abu Bakar NN, Bazmohammadi N, Vasquez JC, Guerrero JM. Electrification of onshore power systems in maritime transportation towards decarbonization of ports: a review of the cold ironing technology. Renew Sustain Energy Rev 2023;178:113243. https://doi.org/10.1016/J.RSER.2023.113243.
[24] Vourdoubas J. The interconnection of the electric grid in the island of Crete, Greece, and its contribution to the clean energy transition. European Journal of Environment and Earth Sciences 2023;4:1–9. https://doi.org/10.24018/ejgeo.2023.4.6.429.
[25] Vourdoubas J. Reduction of CO2 emissions due to energy use in Crete-Greece. Energy Environ Res 2016;6:23. https://doi.org/10.5539/eer.v6n1p23.
[26] Thalassinakis E. Crete power system interconnection-challenges, problems and benefits, n.d. https://www.researchgate.net/publication/385242152_Crete_Power_System_Interconnection-Challenges_problems_and_benefits.
[27] Independent power transmission operator (IPTO), ariadne interconnection, (n.d.). https://www.ariadne-interconnection.gr/en (accessed October 7, 2025).
[28] Vourdoubas J. Islands with zero net carbon footprint due to electricity use. The case of Crete, Greece. European Journal of Environment and Earth Sciences 2021;2:37–43. https://doi.org/10.24018/ejgeo.2021.2.1.116.
[29] Energy planning of the region of Crete. https://www.crete.gov.gr/wp-content/uploads/2023/11/%CE%93-%CE%94-%CE%A0%CE%91%CE%A1%CE%91%CE%94%CE%9F%CE%A4%CE%95%CE%91-09-05-2016_%CE%A4%CE%B5%CE%BB%CE%B9%CE%BA%CF%8C.pdf.
[30] Eunice Group. Greece - africa power interconnector (GAP interconnector) project, (n.d.). https://eunice-group.com/projects/greece-africa-power-interconnector-gap-interconnector/.
[31] Eunice group, Aigaio project, (n.d.). https://eunice-group.com/projects/aigaio-project/(accessed June 9, 2025).
[32] Ajanovic A, Haas R. Prospects and impediments for hydrogen and fuel cell vehicles in the transport sector. Int J Hydrogen Energy 2021;46:10049–58. https://doi.org/10.1016/j.ijhydene.2020.03.122.
[33] Pivetta D, Dall'Armi C, Sandrin P, Bogar M, Taccani R. The role of hydrogen as enabler of industrial port area decarbonization. Renew Sustain Energy Rev 2024;189. https://doi.org/10.1016/j.rser.2023.113912.
[34] Wu Y, Chen A, Xiao H, Jano-Ito M, Alnaeli M, Alnajideen M, Mashruk S, Valera-Medina A. Emission reduction and cost-benefit analysis of the use of ammonia and green hydrogen as fuel for marine applications. Green Energy and Resources 2023;1. https://doi.org/10.1016/j.gerr.2023.100046.
[35] Veldhuis IJS, Richardson RN, Stone HBJ. Hydrogen fuel in a marine environment. Int J Hydrogen Energy 2007;32:2553–66. https://doi.org/10.1016/j.ijhydene.2006.11.013.
[36] Ustolin F, Campari A, Taccani R. An extensive review of liquid hydrogen in transportation with focus on the maritime sector. J Mar Sci Eng 2022;10. https://doi.org/10.3390/jmse10091222.
[37] Peddi KP, Ricci S, Rizzetto L. Reduction potential of gaseous emissions in European ports using cold ironing. Applied Sciences (Switzerland) 2024;14. https://doi.org/10.3390/app14156837.
[38] Abu Bakar NN, Bazmohammadi N, Vasquez JC, Guerrero JM. Electrification of onshore power systems in maritime transportation towards decarbonization of ports: a review of the cold ironing technology. Renew Sustain Energy Rev 2023;178. https://doi.org/10.1016/j.rser.2023.113243.
[39] Sembler WJ, Kumar S, Palmer D. Fuel cells as an alternative to cold ironing. J Fuel Cell Sci Technol 2009;6:310091–3100911. https://doi.org/10.1115/1.3006305.
[40] PyPSA, components, (n.d.). https://docs.pypsa.org/latest/user-guide/components/buses/ (accessed May 27, 2025).
[41] European Commission, Feed-In tariff in Greece, (n.d.). https://clean-energy-islands.ec.europa.eu/countries/greece/legal/electricity-support/feed-tariff.
[42] Marocco P, Gandiglio M, Santarelli M. Optimal design of PV-based grid-connected hydrogen production systems. J Clean Prod 2024;434. https://doi.org/10.1016/j.jclepro.2023.140007.
[43] Aliaksei Patonia. Poudineh Rahmatallah Cost-competitive green hydrogen : how to lower the cost of electrolysers? The Oxford Institute for Energy Studies; 2022. https://www.oxfordenergy.org/publications/cost-competitive-green-hydrogen-how-to-lower-the-cost-of-electrolysers/.
[44] Frazer-Nash Consultancy. Fugitive hydrogen emissions in a future hydrogen economy. 2022. https://assets.publishing.service.gov.uk/media/624ec79cd3bf7f600d4055d1/fugitive-hydrogen-emissions-future-hydrogen-economy.pdf.
[45] Moccia L. Optimization of baseload electricity and hydrogen services by renewables for a nuclear-sized district in South Italy. Smart Energy 2025;17. https://doi.org/10.1016/j.segy.2024.100165.
[46] Electricity maps, (n.d.). https://app.electricitymaps.com/map/72h/hourly (accessed March 12, 2025).
[47] Caponi R, Monforti Ferrario A, Del Zotto L, Bocci E. Hydrogen refueling stations and fuel cell buses four year operational analysis under real-world conditions. Int J Hydrogen Energy 2023;48:20957–70. https://doi.org/10.1016/J.IJHYDENE.2022.10.093.
[48] M. Bampaou, K. Panopoulos, Deliverable 6.6 – WP6. Alternative potential end-use applications and replication studies, n.d.
[49] D'Agostino F, Schiapparelli GP, Dallas S, Spathis D, Georgiou V, Prousalidis J. On estimating the port power demands for cold ironing applications. In: 2021 IEEE electric ship technologies symposium, ESTS 2021. Institute of Electrical and Electronics Engineers Inc.; 2021. https://doi.org/10.1109/ESTS49166.2021.9512359.
[50] JRC, Photovoltaic Geographical Information System (PVGIS), (n.d.). JRC photovoltaic geographical information system (PVGIS) - european commission (accessed May 27, 2025). https://joint-research-centre.ec.europa.eu/photovoltaic-geographical-information-system-pvgis_en.
[51] Danish Energy Agency. Technology data-energy plants for electricity and district heating generation. https://ens.dk/technologydata; 2025.
[52] Jamshidi M, Askarzadeh A. Techno-economic analysis and size optimization of an off-grid hybrid photovoltaic, fuel cell and diesel generator system. Sustain Cities Soc 2019;44:310–20. https://doi.org/10.1016/J.SCS.2018.10.021.
[53] Renewables.ninja, wind database, (n.d.). https://www.renewables.ninja/(accessed May 27, 2025).
[54] Hedno, (n.d.). https://deddie.gr/en/(accessed June 26, 2025).
[55] Ember, European Wholesale Electricity Price Data, (n.d.). European wholesale electricity price data (accessed May 27, 2025). https://ember-energy.org/data/european-wholesale-electricity-price-data/.
[56] Nguyen T, Abdin Z, Holm T, Mérida W. Grid-connected hydrogen production via large-scale water electrolysis. Energy Convers Manag 2019;200:112108. https://doi.org/10.1016/J.ENCONMAN.2019.112108.
[57] Cole W, Frazier AW, Augustine C. Cost projections for utility-scale battery storage: 2021 update. www.nrel.gov/publications; 2021.
[58] Marocco P, Gandiglio M, Santarelli M. When SOFC-based cogeneration systems become convenient? A cost-optimal analysis. Energy Rep 2022;8:8709–21. https://doi.org/10.1016/J.EGYR.2022.06.015.
[59] Böhm H, Zauner A, Rosenfeld DC, Tichler R. Projecting cost development for future large-scale power-to-gas implementations by scaling effects. Appl Energy 2020;264:114780. https://doi.org/10.1016/J.APENERGY.2020.114780.

[60] Tractebel Hinicio Study on early business cases for H2 in energy storage and more broadly power to H2 applications. https://hinicio.com/wp-content/uploads/2022/08/P2H_Full_Study_FCHJU.pdf.
[61] International Renewable Energy Agency. Green hydrogen cost reduction: scaling up electrolysers to meet the 1.50C climate goal, Abu Dhabi. 2020. https://www.irena.org/-/media/Files/IRENA/Agency/Publication/2020/Dec/IRENA_Green_hydrogen_cost_2020.pdf. [Accessed 27 May 2025].
[62] S. Mingolla, K. Rouwenhorst, P. Gabrielli, G. Sansavini, M.M. Klemun, Z. Lu, Optimizing Sustainable Fertilizer Production: Techno-economic and environmental assessment of flexible electrolytic ammonia Production, n.d. https://ssrn.com/abstract=4791664.
[63] Marocco P, Gandiglio M, Audisio D, Santarelli M. Assessment of the role of hydrogen to produce high-temperature heat in the steel industry. J Clean Prod 2023;388:135969. https://doi.org/10.1016/J.JCLEPRO.2023.135969.
[64] Magnino A, Marocco P, Santarelli M, Gandiglio M. Economic viability and CO2 emissions of hydrogen production for ammonia synthesis: a comparative analysis across Europe. Adv Appl Energy 2025;17:100204. https://doi.org/10.1016/J.ADAPEN.2024.100204.
[65] Bravo Diaz L, Weidner E, Dolci F, Georgakaki A, Letout S, Mountraki A, Gea Bermudez J, Wegener M, Schade B. Fuel cell technology in the European Union - 2024 status report on technology development, trends, value chains and markets. Luxembourg: in: Publications Office of the European Union; 2024. https://doi.org/10.2760/0304421.
[66] Marocco P, Ferrero D, Gandiglio M, Ortiz MM, Sundseth K, Lanzini A, Santarelli M. A study of the techno-economic feasibility of H2-based energy storage systems in remote areas. Energy Convers Manag 2020;211:112768. https://doi.org/10.1016/J.ENCONMAN.2020.112768.
[67] Danish Energy Agency. Technology data-energy storage. 2019. https://ens.dk/en/analyses-and-statistics/technology-data-energy-storage.
[68] Rozzi E, Giglio E, Moscoloni C, Novo R, Mattiazzo G, Lanzini A. Comparative study of electric and hydrogen mobility infrastructures for sustainable public transport: a PyPSA optimization for a remote island context. Int J Hydrogen Energy 2024;80:516–27. https://doi.org/10.1016/J.IJHYDENE.2024.07.105.
[69] Viktorsson L, Heinonen JT, Skulason JB, Unnthorsson R. A step towards the hydrogen economy - a life cycle cost analysis of a hydrogen refueling station. Energies (Basel) 2017;10. https://doi.org/10.3390/en10060763.
[70] Atabay R, Devrim Y. Design and techno-economic analysis of solar energy based on-site hydrogen refueling station. Int J Hydrogen Energy 2024;80:151–60. https://doi.org/10.1016/J.IJHYDENE.2024.07.166.